Effect of Three-Phase Relative Permeability on Field-Scale Carbon Dioxide Storage and Oil Recovery

Oranan Ariyarit[a,*] Ann H. Muggeridge[a] Vinicius L. S. Silva[a,b]
Nopparit Somboonkittichai[c] Nattaphon Temkiatvises[d] Martin J. Blunt[a]

[a] Department of Earth Science and Engineering, Imperial College London, UK

[b] Petróleo Brasileiro S.A. (Petrobras), Rio de Janeiro, Brazil

[c] Department of Physics, Kasetsart University, Thailand

[d] PTTEP Energy Development Company Limited, Thailand

* Corresponding author.

Corresponding author:

oranan.ariyarit14@imperial.ac.uk

ORCID: 0009-0002-1098-5184

Preprint notice:

This is a non-peer-reviewed preprint submitted to EarthArXiv. An earlier version of this manuscript was submitted to Geoenergy Science and Engineering for peer review.

Effect of Three-Phase Relative Permeability on Field-Scale Carbon Dioxide Storage and Oil Recovery

Oranan Ariyarit[a] Ann H. Muggeridge[a] Vinicius L. S. Silva[a,b]
Nopparit Somboonkittichai[c] Nattaphon Temkiatvises[d] Martin J. Blunt[a]

[a] Department of Earth Science and Engineering, Imperial College London, UK
[b] Petróleo Brasileiro S.A. (Petrobras), Rio de Janeiro, Brazil
[c] Department of Physics, Kasetsart University, Thailand
[d] PTTEP Energy Development Company Limited, Thailand

Abstract

Currently, the vast majority of subsurface carbon dioxide storage occurs in mature oil fields, where sequestration is combined with enhanced oil recovery. When carbon dioxide is injected below the minimum miscibility pressure, three-phase flow occurs. We study the sensitivity of assumptions made in the assignment of three-phase relative permeabilities on predicted oil recovery and carbon dioxide storage for a three-dimensional reservoir models. We investigate saturation paths, time to water breakthrough, oil recovery and gas storage in weakly water-wet and strongly oil-wet reservoirs, using representative two-phase relative permeabilities. Different interpolation methods to determine the three-phase relative permeabilities are used to assess the impact on reservoir performance. In particular, we show how a physically-consistent characterization of the gas relative permeability has a critical impact on predicted performance. Using saturation-weighted interpolation on the gas relative permeability between gas/oil and gas/water endpoints, where gas is not the most non-wetting phase in the presence of mobile water, has a major impact on CO_2 storage: compared to a traditional model using only the gas/oil relative permeability 10% more CO_2 is stored, while the oil recovery is 5% lower. This work stresses the necessity of having accurate measurements of relative permeability when assessing CO_2 storage in oil fields, and the importance of allowing all three relative permeabilities to vary as a function of two independent saturations.

1 Introduction

Carbon dioxide storage is a key component of efforts to reach net zero carbon emissions (Shu et al., 2023)(Burger et al., 2024). At present the vast majority of carbon dioxide storage occurs in oil fields due to the economic benefit of additional hydrocarbon recovery, the availability of existing injection infrastructure and the guarantee of a secure cap rock (Whittaker and Perkins, 2013)(Roussanaly and Grimstad, 2014)(Longe et al., 2025)(National Petroleum Council, 2021)(Mirzaei-Paiaman et al., 2024). Traditionally, the reason for injecting carbon dioxide was to increase oil recovery. Carbon dioxide is typically injected with water – water alternate gas injection, WAG – to reduce the mobility contrast between the injected fluids and resident oil, to increase the volume of the reservoir contacted, and to reduce costs. Furthermore, the injection pressure is often sufficiently high such that the carbon dioxide and oil are miscible – they form a single phase – as this leads to complete displacement of oil locally. If the carbon dioxide comes at a cost, the most efficient design involves retaining as little of the gas in the subsurface as possible; instead carbon dioxide is produced, separated from the oil and then reinjected.

If there are direct incentives or tax credits associated with permanent sequestration of carbon dioxide, then the injection design needs to be modified to retain as much injected gas underground as possible. It may therefore be desirable to inject less water than in recovery-focused operations, or inject at a lower pressure where carbon dioxide and oil form distinct phases. In such cases, the flow properties of the gas become important and need to be characterized accurately to predict the movement and storage of carbon dioxide.

Traditionally, the gas relative permeability is measured in the presence of oil with irreducible water. In this case, gas is always the most non-wetting phase, occupies the largest pores and has a high relative permeability once the gas connects across the sample Blunt (2017). However, with mobile water present, it is possible that in an oil-wet or mixed-wet rock, the water is the most non-wetting phase. The water blocks the larger pores, while gas is confined to spreading layers or pores of intermediate size. It may also be poorly connected in the pore space. This is particularly true for near-miscible displacements, when the interfacial and wetting properties of the oil and gas become similar (Alhosani et al., 2021). Hence it is likely that current models over-estimate the gas relative permeability (Foroudi et al., 2022)(Masalmeh et al., 2025) leading to erroneous assessments of gas storage; in particular models may exaggerate the migration of gas, and how much is reproduced while under-estimating the net amount retained underground.

Many studies have shown that the correct relative permeability model is necessary to make accurate field-scale predictions (Hustad, 2002)(Hustad and Browning, 2010)(Shahverdi et al., 2012)(Foroudi et al., 2022)(Masalmeh et al., 2025)(Jerauld, 1997a)(Guzman et al., 1994)(Acharya et al., 2024)(Qi et al., 2009)(Qi et al., 2008)(Brown, 2014). In three-phase flow, a challenge is to interpolate the behavior seen in experiments when only two phases are mobile (oil and water, gas and oil, or gas and water) to cases where all three phases can flow.

In general, interpolation methods are only implemented for the oil-phase relative permeabilities from gas/oil and water/oil systems Stone (1970). It is rare to interpolate gas relative permeabilities between gas/oil and gas/water displacement, and water relative permeabilities between water/oil, and water/gas experiments.

In this study, we use interpolation methods for all three-phase relative permeabilities – CO_2 gas, oil, and water – to illustrate the impact of three-phase relative permeability on CO_2 storage capacity and oil recovery. We explore how physically-justified assumptions of a low CO_2 relative permeability in the presence of mobile water affects field-scale predictions of trapping and recovery. We show that using a more accurate representation of the gas relative permeability leads to predictions of more storage. Furthermore, we show that it is possible to design effective injection schemes without the use of water injection.

2 Method

The studies were divided into two main parts: the sensitivity of predcitions of recovery and storage on interpolation methods for only one phase, oil, and the sensitivity using interpolation methods on all three phases – CO_2 gas, oil, and water.

2.1 Interpolation Methods for Relative Permeability

Three-phase oil relative permeabilities are estimated from measurements on oil/water and oil/gas systems with only two mobile phases present. Interpolation methods are used to combine these two sets of data. In this work we will consider the Stone I (Stone, 1970), Baker (Baker, 1988) and Hustad et al. (Hustad and Hansen, 1995)(Hustad et al., 2002) models. We also note that other models have been proposed extending these interpolation methods, but these will not be considered here: (Stone, 1973; Aziz and Settari, 1979; Delshad and Pope, 1989; Jerauld, 1997b; Moulu et al., 1997; Blunt, 2000; Hustad and Browning, 2010; Shahverdi and Sohrabi, 2013, 2015, 2017; Schäfer et al., 2020; Beygi et al., 2015).

2.1.1 Stone I

The Stone I model is usually implemented on only the oil phase. The relative permeabilities of gas and water are assumed to be equal to the relative permeability in gas/oil and water/oil systems, respectively based on the usually erroneous assumption that the reservoir is water-wet.

The Stone I equations are as follows (Blunt, 2017) modified to allow the oil relative permeabilities to reach the correct two-phase limit at the maximum oil saturation (Shahverdi and Sohrabi, 2017):

$$k_{ro} = \frac{S_{oe}\, k_{ro(w)}(S_w)\, k_{ro(g)}(S_g)}{k_{ro}^{\max}(1 - S_{we})(1 - S_{ge})} \tag{1}$$

$$S_{oe} = \frac{S_o - S_{om}}{(1 - S_{wc} - S_{om})} \tag{2}$$

$$S_{we} = \frac{S_w - S_{wc}}{(1 - S_{wc} - S_{om})} \tag{3}$$

$$S_{ge} = \frac{S_g}{(1 - S_{wi} - S_{om})} \tag{4}$$

where S_{om} is the residual oil saturation, which can be determined using linear interpolation or empirical correlations. Here, S_{om} is specified as 0.10 for the oil-wet rock and 0.18 for the weakly water-wet rock.

2.1.2 Baker

The Baker model is a saturation-weighted interpolation method. The oil relative permeabilities are sampled from two-phase flow values at each oil saturation. The Baker model can be implemented in all phases: gas, oil, and water. It makes no particular assumptions concerning reservoir wettability. The equations of the Baker model are (Blunt, 2017):

$$k_{ro} = \frac{(S_w - S_{wi})k_{ro(w)}(S_o) + (S_g - S_{gr})k_{ro(g)}(S_o)}{(S_w - S_{wi}) + (S_g - S_{gr})} \tag{5}$$

$$k_{rw} = \frac{(S_o - S_{oi})k_{rw(o)}(S_w) + (S_g - S_{gr})k_{rw(g)}(S_w)}{(S_o - S_{oi}) + (S_g - S_{gr})} \tag{6}$$

$$k_{rg} = \frac{(S_w - S_{wi})k_{rg(w)}(S_g) + (S_o - S_{oi})k_{rg(o)}(S_g)}{(S_w - S_{wi}) + (S_o - S_{oi})} \tag{7}$$

2.1.3 Hustad et al.

The Baker model was extended by Hustad et al. using the IKU3P method Hustad (2002). The relative permeabilities of each phase are controlled by the mobile saturation of each phase and not the total saturation. The effective saturation ranges of each phase are interpolated linearly based on residual saturations which are derived from two-phase relative permeabilities. For example, the oil saturation is normalized between the lowest value which is estimated between $S_{or(w)}$ and $S_{or(g)}$ and the highest value which is estimated between $S_{wr(o)}$ and $S_{gr(o)}$.The equations for the IKU3P method are as follows (Shahverdi et al., 2012):

$$S_{omn} = \frac{S_w S_{orw} + S_g S_{org} + S_{org} S_{orw}(S_o - 1)}{S_g(1 - S_{orw}) + S_w(1 - S_{org})} \tag{8}$$

$$S_{omx} = \frac{S_w S_{gro} + S_g S_{wro} + S_{gro} S_{wro}(S_o - 1)}{S_g S_{wro} + S_w S_{gro}} \tag{9}$$

$$S_o^* = \frac{S_o - S_{omn}}{S_{omx} - S_{omn}} \tag{10}$$

$$\hat{k}_{rog} = k_{rog}^n(S_o^*) \tag{11}$$

$$\hat{k}_{row} = k_{row}^n(S_o^*) \tag{12}$$

where n indicates an empirical exponent, $\hat{k}_{rog}$ represents the normalized oil relative permeability in the presence of gas at normalized oil saturation, and $\hat{k}_{row}$ represents the normalized oil relative permeability in the presence of water at normalized oil saturation. The interpolated oil relative permeabilities are then calculated using the equation below, see Fig. 1.

$$k_{ro} = \frac{S_w}{S_w + S_g}\hat{k}_{row} + \frac{S_g}{S_w + S_g}\hat{k}_{rog} \tag{13}$$

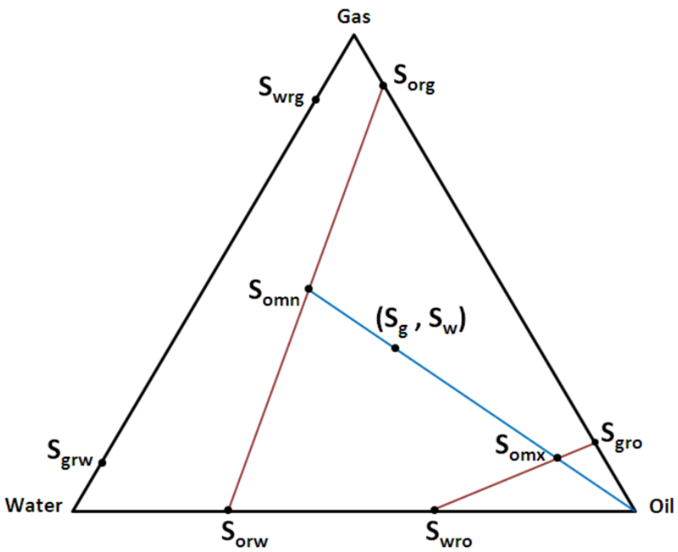

Fig. 1: A schematic showing how to evaluate the normalized saturation in the IKU3P model (Shahverdi et al., 2012).

2.2 Relative Permeability Models

We considered relative permeabilities representative of either an oil-wet or weakly water-wet reservoir. The equations for the Corey-type relative permeabilities are presented in Equations (14) – (19). The endpoint values and relative permeability assumptions are shown in Table 1 – 3. The relative permeabilities are shown in Figs. 2 and 3.

Equations for oil/water systems:

$$k_{rw(o)}(S_w) = k_{rw}^{\max}\left(\frac{S_w - S_{wi}}{1 - S_{wi} - S_{or(w)}}\right)^a \tag{14}$$

$$k_{ro(w)}(S_w) = k_{ro}^{\max}\left(\frac{1 - S_{or(w)} - S_w}{1 - S_{wi} - S_{or(w)}}\right)^b \tag{15}$$

Equations for gas/oil systems:

$$k_{rg(o)}(S_g) = k_{rg}^{\max}\left(\frac{S_g - S_{gc}}{1 - S_{wi} - S_{or(g)} - S_{gc}}\right)^c \tag{16}$$

$$k_{ro(g)}(S_g) = k_{ro}^{\max}\left(\frac{1 - S_{wi} - S_{or(g)} - S_g}{1 - S_{wi} - S_{or(g)} - S_{gc}}\right)^d \tag{17}$$

Equations for gas/water systems:

$$k_{rw(g)} = k_{rw}^{\max}\left(\frac{S_w - S_{wi}}{1 - S_{wi}}\right)^e \tag{18}$$

$$k_{rg(w)} = k_{rg}^{\max}\left(\frac{1 - S_w}{1 - S_{wi}}\right)^f \tag{19}$$

Table 1: Parameters for oil/water systems

Parameter	Weakly water-wet	Oil-wet
$S_{or(w)}$	0.3	0.15
S_{wi}	0.2	0.2
$k_{rw}^{\max}$	0.2	0.6
a	3	1.5
$k_{ro}^{\max}$	0.9	0.9
b	1.5	4

Table 2: Parameters for gas/oil systems

Parameter	Value
S_{wi}	0.2
S_{gc}	0
$S_{or(g)}$	0
$k_{rg}^{\max}$	0.9
c	1
$k_{ro}^{\max}$	0.9
d	5

Table 3: Parameters for gas/water systems

Parameter	Value
S_{wi}	0.2
$k_{rw}^{\max}$	1
e	1.5
$k_{rg}^{\max}$	0.9
f	5

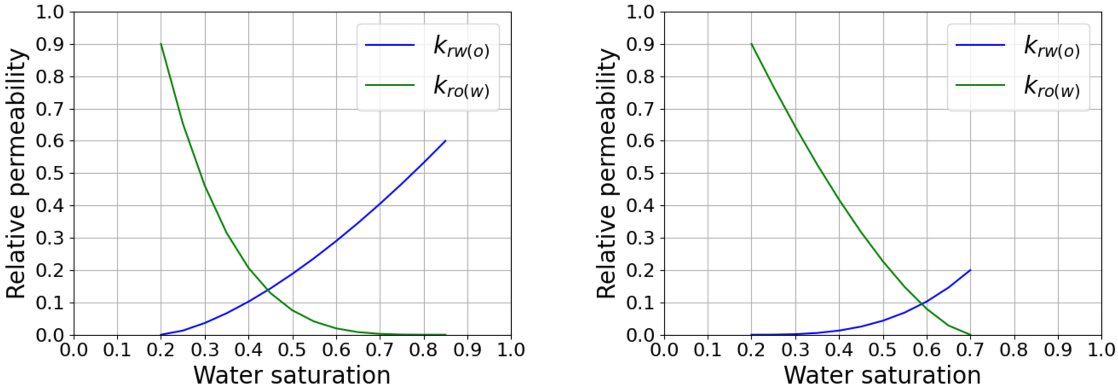

Fig. 2: Oil/water relative permeabilities in oil-wet (left) and weakly water-wet rocks (right).

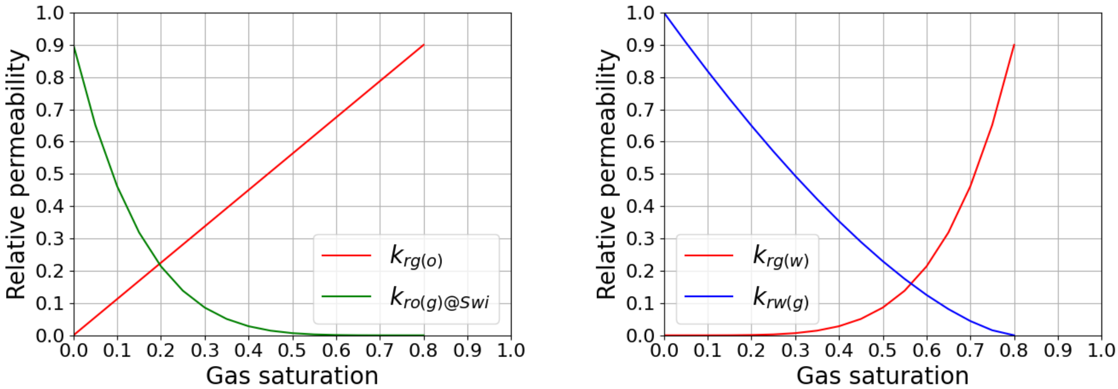

Fig. 3: Gas/oil (left) and gas/water (right) relative permeabilities in both oil-wet and weakly water-wet rocks.

2.3 Three-Dimensional Model

A simplified reservoir model was constructed representative of a homogeneous sandstone reservoir. The domain was 7,315 m in length, 4,877 m in width, and at a depth between 884 and 975 m. The model had 96,000 active grid cells. The cell size was 61 x 61 x 9 m. An inverted 5-spot well pattern was used. There were 16 producers and 9 injectors. The injectors were used for both water and gas injection.

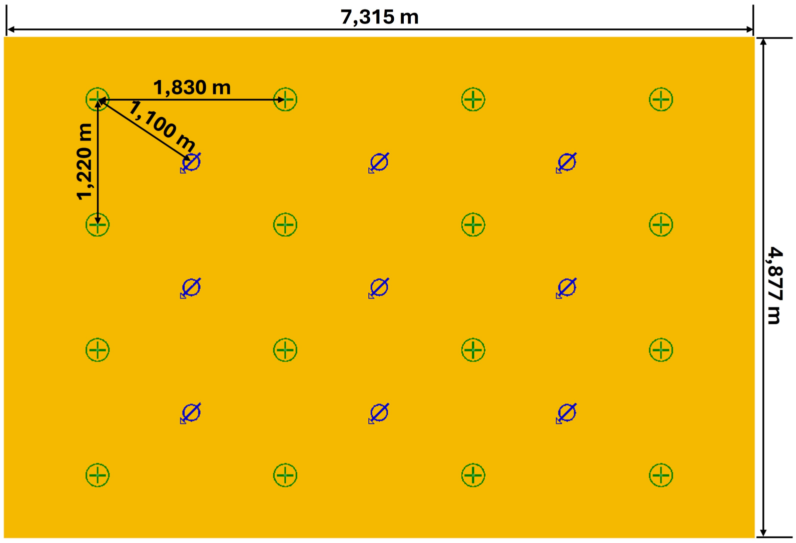

Fig. 4: Domain and well placement in the 3D model.

A light oil fluid model was used. Initial reservoir pressure was 26.2 MPa. The bubble point pressure was 25.8 MPa. The temperature was 107°C. The oil-water contact was at a depth of 975 m. Permeabilities in the x- and y-directions were 100 mD, while in the z-direction it was 10 mD. Porosity was 25%. ECLIPSE E300 was used as the simulator.

For the field development plan, water was injected first, followed by gas injection. Water was injected at around 40% to 50% of pore volume to ensure that it broke through to the producers. Water injection rates were calculated from pore volume and the number of injectors. Production rates were calculated using material balance and the ratio of the number of injectors to producers. Gas injection rates were set to maintain the reservoir pressure. The input rates in the simulator were increased slightly to allow reservoir rate control and bottom hole pressure control modes to be independent from the effect of various interpolation methods. Details are illustrated below.

Table 4: Injection schedule over 40 years for oil-wet rock and 80 years for weakly water-wet rock

	Water injection (20/60 years)		CO_2 injection (20 years)	
	Water injectors	Producers	Gas injectors	Producers
Bottom hole pressure [MPa]	34.5	25.9	34.5	25.9
Surface rate [m^3/d]	8,200	4,700	2,200,000	4,700
Reservoir volume rate [rm^3/d]	8,200	4,600	8,800	4,600

Ternary diagrams of each interpolation method were constructed to understand relative permeabilities in the three-phase region. This will be considered along with the field-scale simulation results.

There were 6 scenarios studied as illustrated in Figure 5.

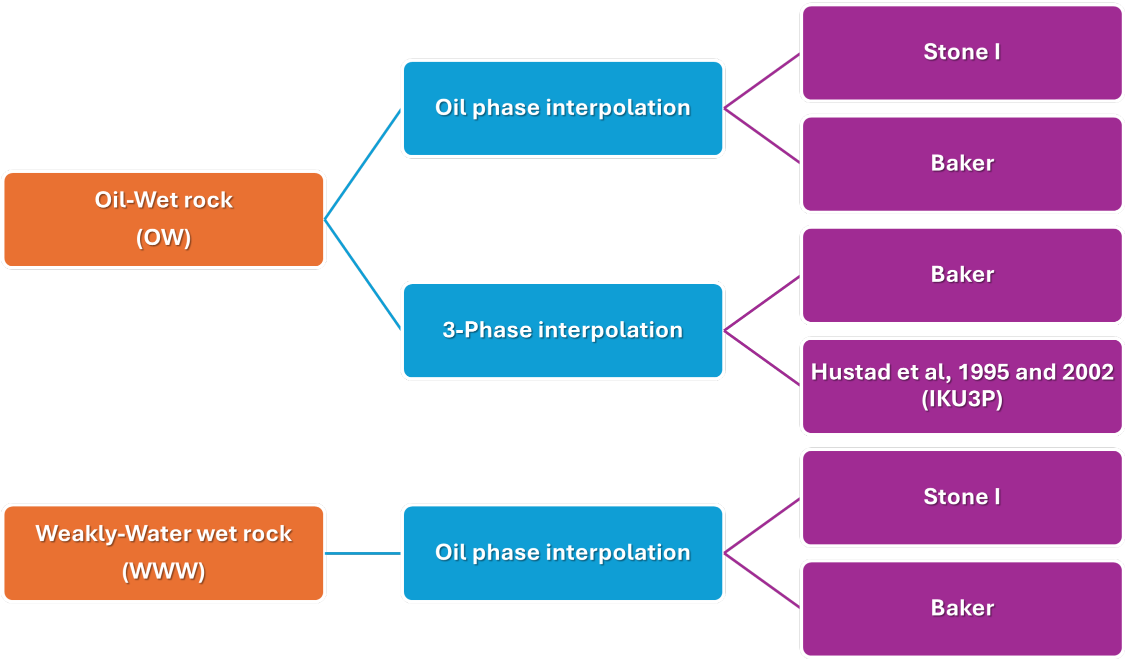

Fig. 5: Sensitivity scenarios.

3 Results and Discussion

3.1 Quality Check

After running simulations, the results were verified to meet the following criteria:

- Water broke through to the producers before the beginning of gas injection.
- Reservoir and bottomhole pressures remained above the bubble point pressure throughout the simulations.

3.2 Oil phase interpolation in weakly water-wet cases

In a weakly water-wet system, the relative permeability of water in the presence of oil is lower compared to an oil-wet case. This causes the volumetric flow rate of water to be lower, subsequently requiring more time for water to breakthrough, as shown in Figure 6.

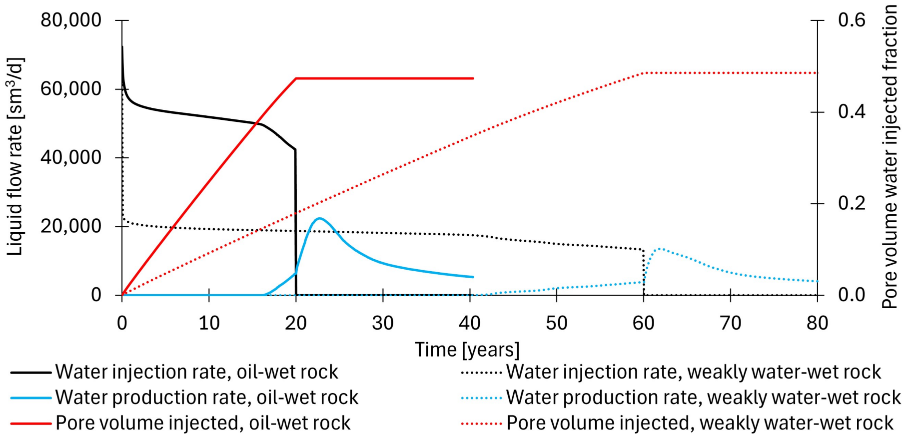

Fig. 6: Fraction of pore volume water injected, and water injection rates compared between oil-wet and weakly-water wet reservoirs.

During water injection, both the Stone I and Baker models show similar oil production rates. However, after gas injection, the differences in oil relative permeabilities lead to changes in behavior. Because the k_{ro} in the Stone I model gradually enters the immobile zone at the start of gas injection as shown in Figure 8, the oil production peak is lower than using the Baker model as shown in Figure 7. In contrast, the Baker model enters the immobile zone immediately that allows some oil flow before entering the immobile zone as shown in Figure 8, which subsequently results in higher oil production rate before it declines and gas breaks through as shown in Figure 7. In both cases, gas breakthroughs occur early due to the higher value of $k_{rg(o)}$ compared to $k_{rw(o)}$, as shown in Figure 9.

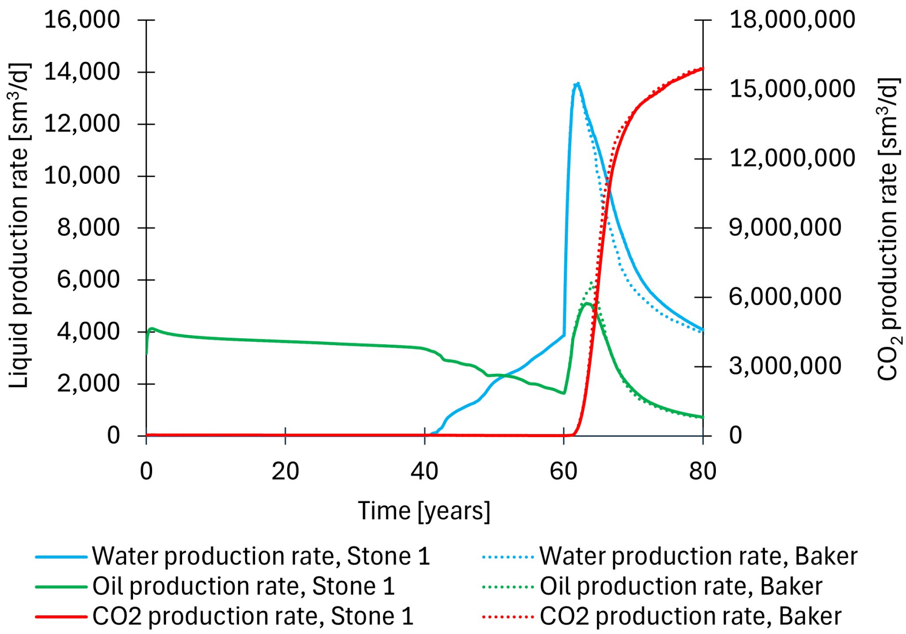

Fig. 7: Three-phase production rates from implementing interpolation of the oil phase using the Baker and Stone I models.

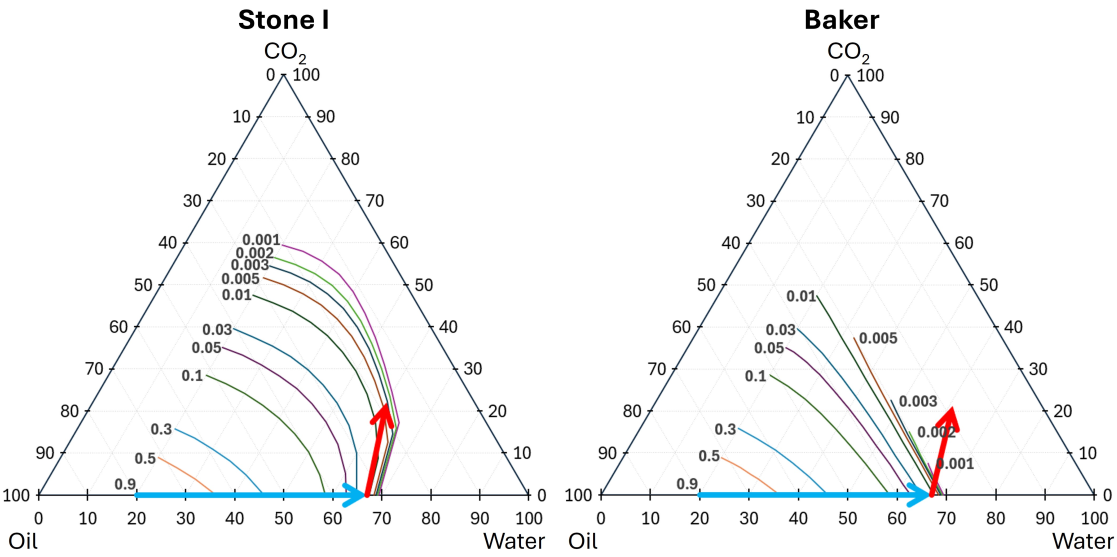

Fig. 8: Ternary diagram with various iso-oil relative permeabilities using Stone I and Baker. Blue arrows represent changes in saturation during water injection, while red arrows represent changes in saturation during gas injection.

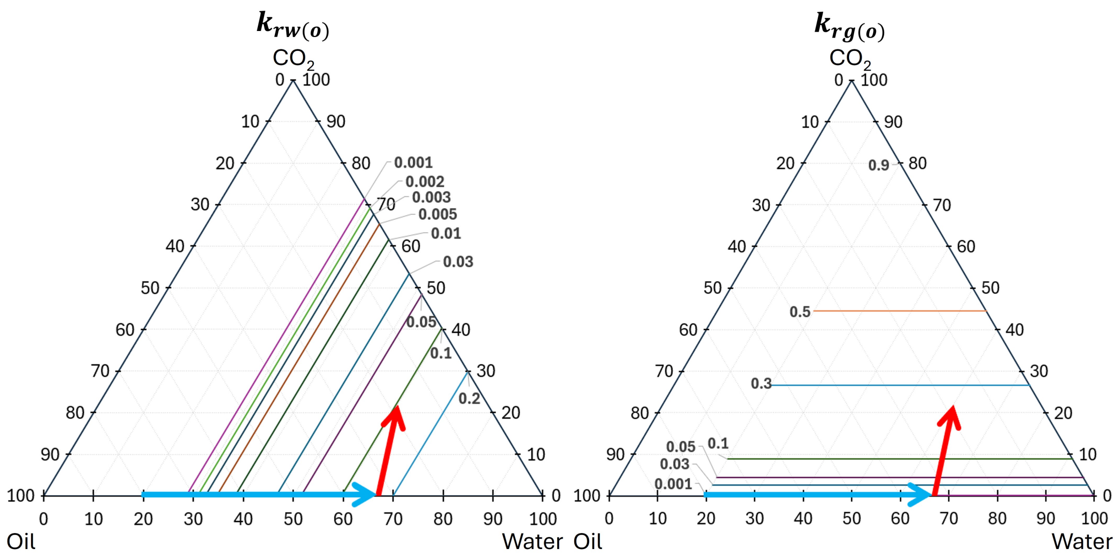

Fig. 9: Ternary diagram with various iso-water and gas relative permeabilities without using interpolation methods. Blue arrows represent changes in saturation during water injection, while red arrows represent changes in saturation during gas injection.

3.3 Oil phase interpolations in oil-wet cases

From Figure 10 and 11, interpolations of oil relative permeability show the impact at the field scale during gas injection. From the ternary diagram, the results from the Baker model pass through the highly mobile oil zone earlier than the Stone I model during early gas injection, which is illustrated by higher oil production between the years 20 to 24. The oil relative permeability in the ternary diagram reaches the immobile oil zone before the Stone I model. This is illustrated by the rapid drop in oil production rate between the years 24 and 28. As the Baker model reaches the immobile oil zone earlier, the gas flow rate becomes dominant and results in earlier gas breakthrough compared to the Stone I model. During gas injection, the processes at the pore scale align with those at the field scale as shown in Figure 11 and 12: k_{ro} decreases, k_{rw} decreases, while k_{rg} increases. These are consistent with a decrease in oil and water production rates and an increase in gas production rates as shown in Figure 10.

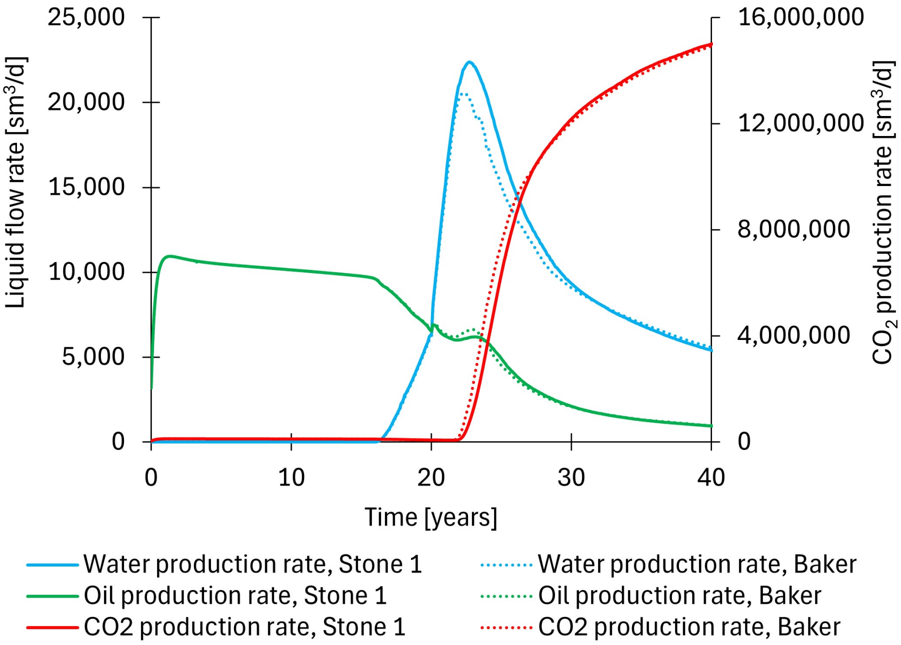

Fig. 10: Three-phase production rates from implementing interpolation of the oil phase using the Baker and Stone I models.

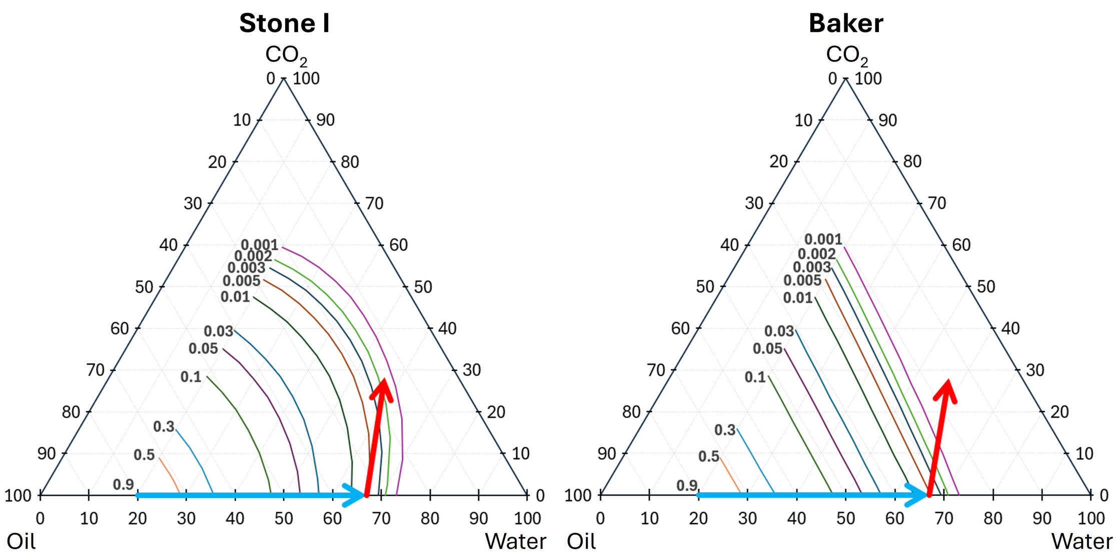

Fig. 11: Ternary diagram with various iso-oil relative permeabilities using Stone I and Baker. Blue arrows represent changes in saturation during water injection, while red arrows represent changes in saturation during gas injection.

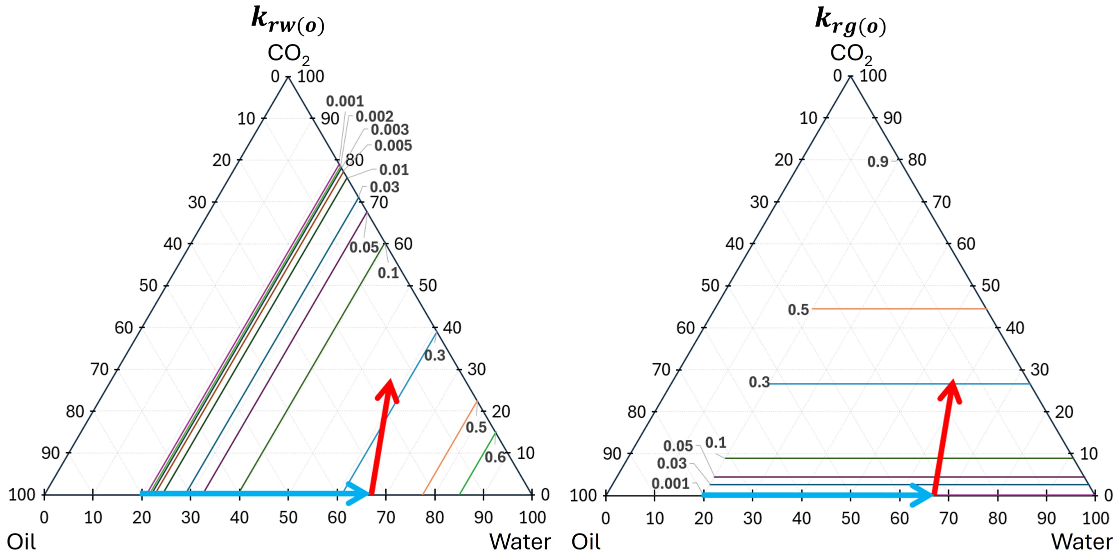

Fig. 12: Ternary diagram with various iso-water and gas relative permeabilities without using interpolation methods. Blue arrows represent changes in saturation during water injection, while red arrows represent changes in saturation during gas injection.

3.4 Effect of three-phase interpolation using the Baker model in oil-wet cases

Overall, the use of three-phase interpolation changes saturation paths during both the water injection and gas injection periods. During water injection, the use of oil phase interpolation reduces oil saturation from 80% to 33%, whereas the use of three-phase interpolation reduces the oil saturation only to 37% as shown in Figures 11 (right) and 14 (left). This creates a significant discrepancy in the field-scale simulation as shown in Figure 13.

At the end of the water injection period (year 20) as shown in Figure 13, with the use of oil phase interpolation only (one-phase interpolation), oil flow still dominates, and water breaks through after the three-phase interpolation case. The k_{ro} of the oil phase interpolation case has already passed through the highly mobile oil region and reached the immobile zone earlier as shown in Figures 11 (right) and 14 (left). These are illustrated at the field scale in Figure 13, where the oil production rate in the oil phase interpolation case is higher during early gas injection and then drops rapidly before the three-phase interpolation case declines. After the oil relative permeability in the oil phase interpolation case approaches the immobile zone, gas breakthrough also occurs earlier.

In addition, the use of the Baker method shifts the gas mobile region at low oil saturation to occur slower as shown in Figures 12 (right) and 16 (left). The slope of the gas production rate in the oil phase interpolation case is also steeper. Therefore, in the three-phase interpolation case, gas moves slower and breaks through later, subsequently storing more CO_2 underground.

From the perspective of water relative permeability, although in the oil phase interpolation case, water breaks through later with a higher $k_{rw(o)}$ as shown in Figures 12 (left) and 15 (left), oil flow still dominates, resulting in a lower water production rate as shown in Figure 13.

In the Baker method, we also found that the greater the difference between end points the more curvature there is in the iso-relative permeability lines as illustrated in Figures 12 (right) and 16 (left).

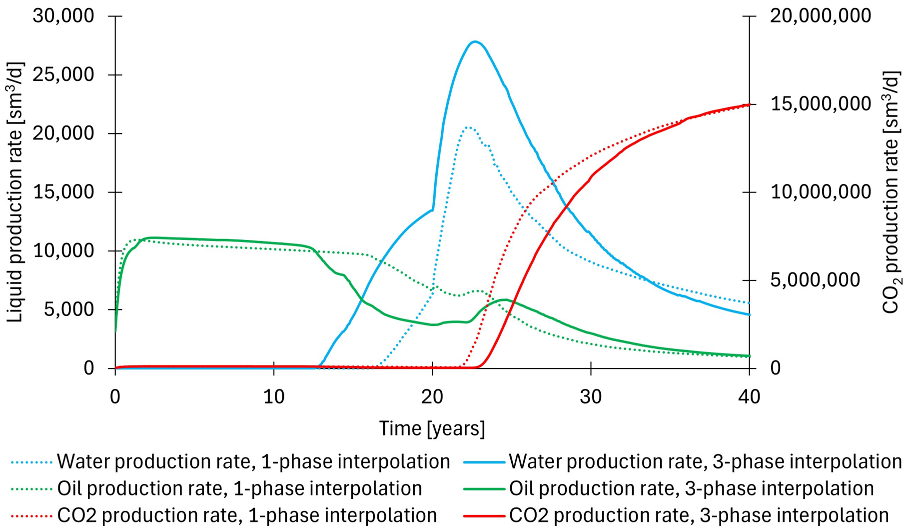

Fig. 13: Comparison of production profiles between oil phase interpolation only and interpolation for all three phases using the Baker model.

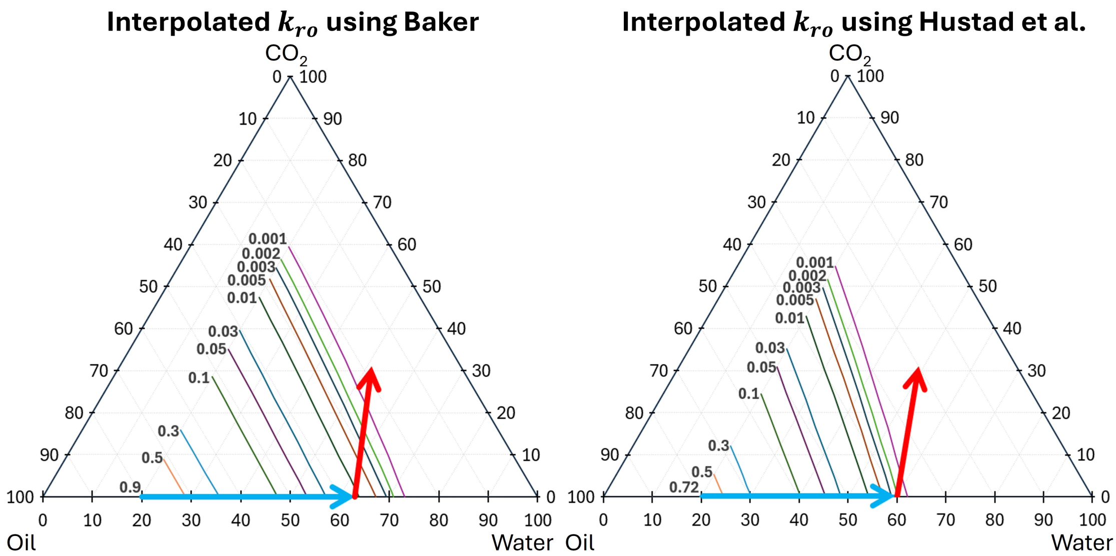

Fig. 14: Iso-oil relative permeabilities and saturation change paths compared between the Baker and Hustad models. Blue arrows represent changes in saturation during water injection, while red arrows represent changes in saturation during gas injection.

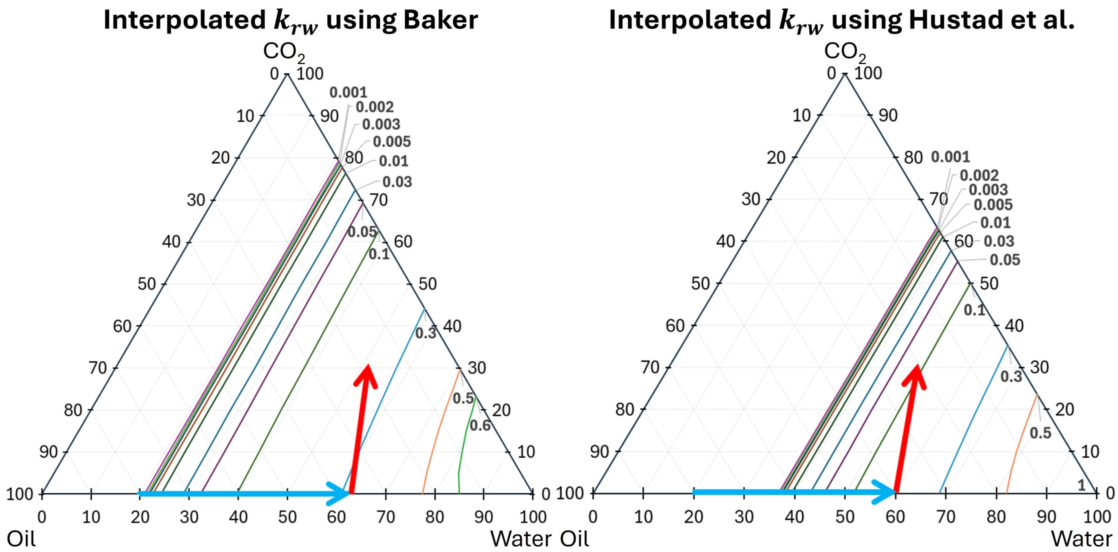

Fig. 15: Iso-water relative permeabilities and saturation change paths compared between the Baker and Hustad models. Blue arrows represent changes in saturation during water injection, while red arrows represent changes in saturation during gas injection.

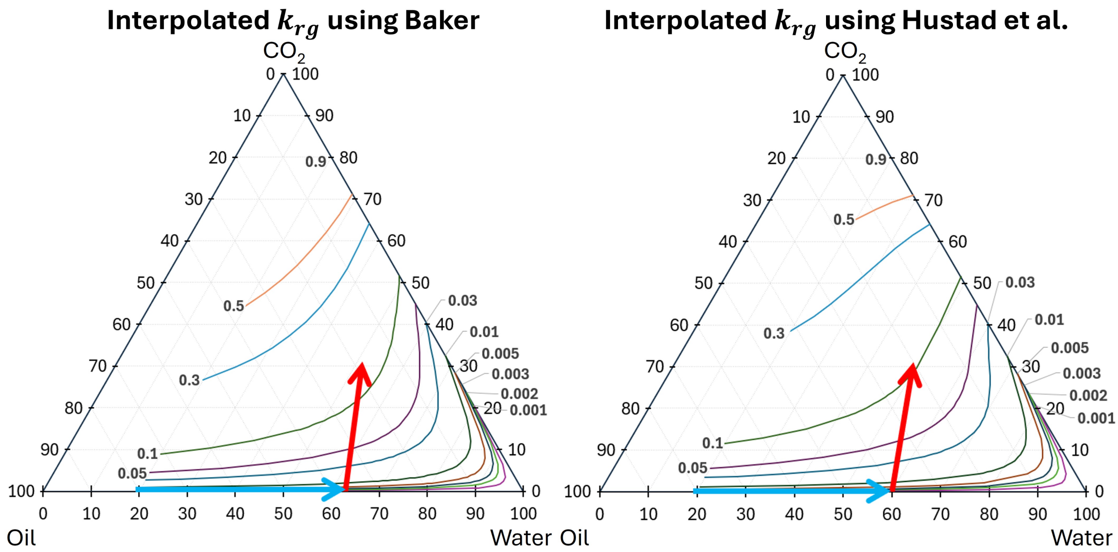

Fig. 16: Iso-gas relative permeabilities and saturation change paths compared between the Baker and Hustad models. Blue arrows represent changes in saturation during water injection, while red arrows represent changes in saturation during gas injection.

3.5 Three-Phase interpolations in oil-wet cases

Here we consider the Hustad et al. model as described in section 2. From Figure 14, during water injection, the relative permeability of oil in the Baker model is higher than in the Hustad model. This causes a higher oil production rate in the Baker model at the start of water injection as shown in Figure 17. Consequently, the Baker model enters the water breakthrough period before the Hustad model. Moreover, because the Baker model has a higher k_{rw} compared to the Hustad model, and the Hustad model has a large zone of immobile water as shown in Figure 15, the Baker model produces more water than the Hustad model.

In terms of gas relative permeability,the Hustad models change the curvatures at high iso-gas relative permeabilities as shown in Figure 16. However, the change in saturation paths only moves through the low gas relative permeability zone. Thus, the gas production profiles of both the Baker and Hustad models are nearly aligned.

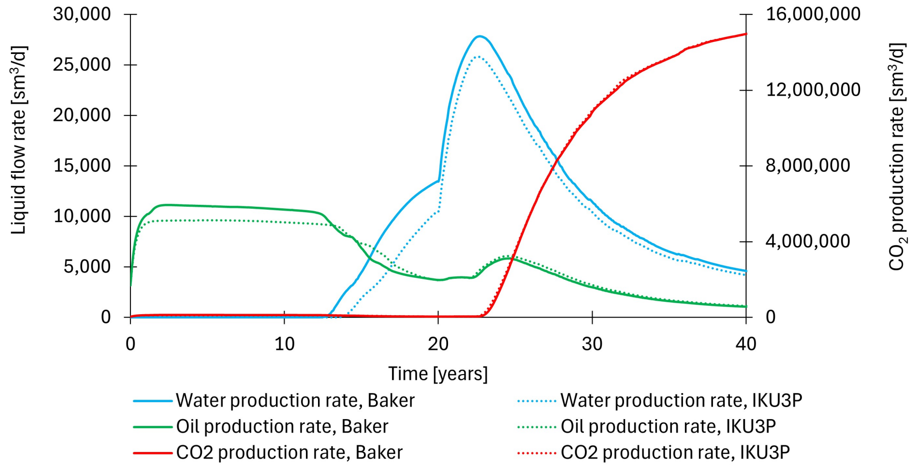

Fig. 17: Comparison of production profiles when using three-phase interpolation. The interpolation methods include the Baker and Hustad et al. models.

From Figure 18, when the oil relative permeability is interpolated, weakly water-wet cases show greater differences between Stone I and the Baker model in both the fraction of the original oil in place recovered, Rf, and the amount of CO_2 storage compared to the oil-wet cases. This is due to larger differences between $k_{ro(w)}$ and $k_{ro(g)}$. In addition, oil-wet cases produce more oil, which indicates better displacement efficiency of water and gas – non-wetting phases – in oil-wet systems as well as resulting in more pore space to store CO_2 underground.

Although oil phase interpolation is important, interpolation in all phases, particularly gas, is more significant and has a greater impact, as discussed in section 3.4, which shows that using oil phase interpolation only results in higher predicted oil recovery. Since oil flow still dominates, water production is lower in the oil phase interpolation case. However, in terms of gas relative permeabilities, the Baker model shifts the low gas relative permeabilities at low oil saturation. Hence, the three-phase interpolation cases predict more CO_2 storage.

The significance of these results is to highlight the importance of having an accurate and physically-consistent model for the gas relative permeability. While the necessity of an appropriate model for the oil relative permeability has been demonstrated previously Guzman et al. (1994), this study shows that in terms of both oil recovery and CO_2 storage, different approximations for the gas relative permeability have an even larger effect.

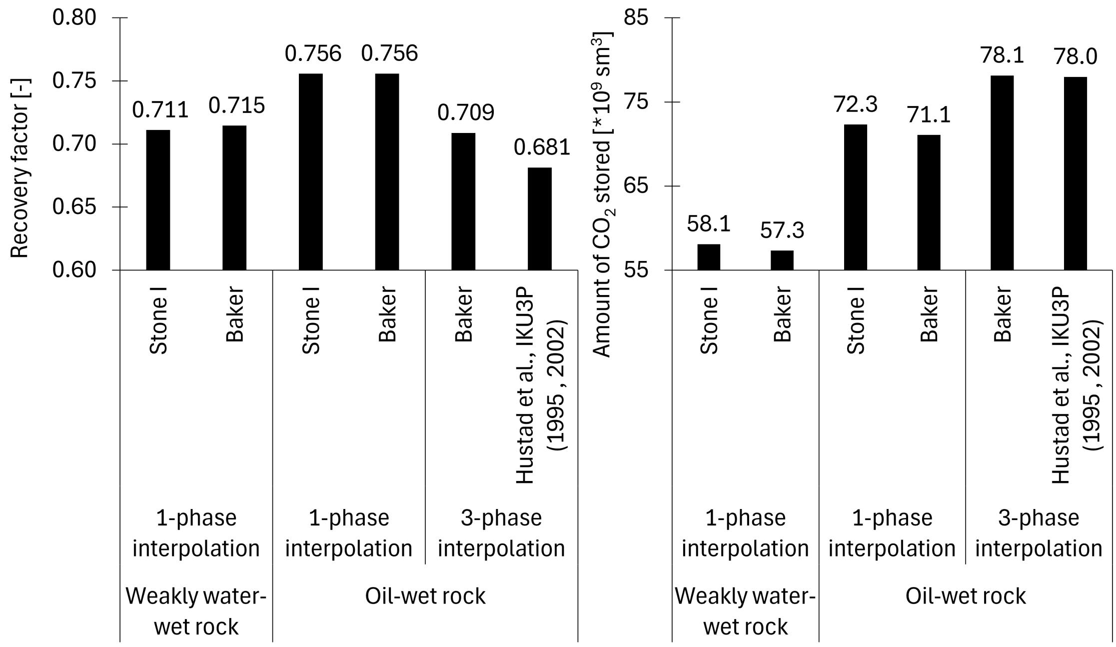

Fig. 18: Comparison of oil recovery factor and amount of CO_2 storage.

4 Conclusions

The study illustrates the importance of the accurate assignment of relative permeabilities and interpolation methods in field-scale simulation. Two types of wettability – weakly water-wet and oil-wet systems – with corresponding representative relative permeabilities were applied to a homogeneous 3D reservoir model. The sensitivity of oil recovery and CO_2 storage to different relative permeability models was explored using the Stone I model for oil relative permeability, and the Baker and Hustad et al. models for interpolation of water, gas, and oil relative permeabilities.

In this context, ternary diagrams, which illustrate the paths of saturation changes and the behavior of iso-relative permeability from various empirical correlations, were compared with field-scale outputs including production profiles, recovery factor, and the amount of trapped CO_2. The evaluation criteria included how fast water breaks through, how efficient the displacement process is, and how saturation changes throughout the simulations.

The principal new finding in this work was the sensitivity of predicted oil recovery and CO_2 storage on the assumptions made concerning gas relative permeability. Traditionally, the gas relative permeability is measured for displacement of oil with immobile water: in this case, gas is the non-wetting phase and once connected through the pore space has a high relative permeability. However, when mobile water is present, in most oilfield settings, water becomes the most non-wetting phase, while gas is intermediate-wet Alhosani et al. (2021). This means that the gas relative permeability is lower in the presence of mobile water, than when displacing oil alone. To capture this behavior a model that extrapolates the gas relative permeability between gas/oil and gas/water two-phase flow is required. Our results show that using this more realistic formulation, the predicted oil recovery is lower, but more CO_2 is retained in the subsurface. This may be an important consideration for the design of CO_2 storage, where a target volume must be stored, or increased retention is associated with additional revenue.

Funding

This work was supported by the Department of Mineral Fuels, Ministry of Energy, Thailand, through a PhD scholarship awarded to Oranan Ariyarit. The funder had no role in the study design, data analysis, interpretation of results, writing of the manuscript, or decision to submit the article for publication.

References

Acharya, T., Dhaliwal, T., Ludian, A., Popli, G., Wilemon, B., Hernandez, L., Farahani, M., and Song, L. (2024). Evaluation of co2/water imbibition relative permeability curves in sandstone core flooding—a cfd study. *Processes*, 12(10):2176.

Alhosani, A., Bijeljic, B., and Blunt, M. J. (2021). Pore-scale imaging and analysis of wettability order, trapping and displacement in three-phase flow in porous media with various wettabilities. *Transport in Porous Media*, 140(1):59–84.

Aziz, K. and Settari, A. (1979). *Petroleum Reservoir Simulation*. Applied Science Publishers, London. Reprinted as Kindle Edition, 2021.

Baker, L. E. (1988). Three-phase relative permeability correlations. volume SPE Enhanced Oil Recovery Symposium of *SPE Improved Oil Recovery Conference*, pages SPE–17369–MS.

Beygi, M. R., Delshad, M., Pudugramam, V. S., Pope, G. A., and Wheeler, M. F. (2015). Novel three-phase compositional relative permeability and three-phase hysteresis models. *SPE Journal*, 20(01):21–34.

Blunt, M. J. (2000). An empirical model for three-phase relative permeability. *Spe Journal*, 5(04):435–445.

Blunt, M. J. (2017). *Multiphase flow in permeable media: A pore-scale perspective*. Cambridge university press.

Brown, J. S. (2014). *A compositional simulation model for carbon dioxide flooding with improved fluid trapping*. Colorado School of Mines.

Burger, J., Nöhl, J., Seiler, J., Gabrielli, P., Oeuvray, P., Becattini, V., Reyes-Lúa, A., Riboldi, L., Sansavini, G., and Bardow, A. (2024). Environmental impacts of carbon capture, transport, and storage supply chains: Status and the way forward. *International Journal of Greenhouse Gas Control*, 132:104039.

Delshad, M. and Pope, G. A. (1989). Comparison of the three-phase oil relative permeability models. *Transport in porous media*, 4(1):59–83.

Foroudi, S., Gharavi, A., and Fatemi, M. (2022). Assessment of two-phase relative permeability hysteresis models for oil/water, gas/water and gas/oil systems in mixed-wet porous media. *Fuel*, 309:122150.

Guzman, R. E., Giordano, D., Fayers, F. J., Aziz, K., and Godi, A. (1994). Three-phase flow in field-scale simulations of gas and wag injections. In *European Petroleum Conference*, pages SPE–28897–MS, London, United Kingdom. Society of Petroleum Engineers.

Hustad, O. and Hansen, A. (1995). A consistent correlation for three phase relative permeabilities and phase pressures based on three sets of two phase data.

Hustad, O. S. (2002). A coupled model for three-phase capillary pressure and relative permeability. *SPE Journal*, 7(01):59–69.

Hustad, O. S. and Browning, D. J. (2010). A fully coupled three-phase model for capillary pressure and relative permeability for implicit compositional reservoir simulation. *SPE Journal*, 15(04):1003–1019.

Hustad, O. S., Kløv, T., Lerdahl, T. R., Berge, L. I., Stensen, J. Å., and Øren, P.-E. (2002). Gas segregation during wag injection and the importance of parameter scaling in three-phase models. volume SPE/DOE Improved Oil Recovery Symposium of *SPE Improved Oil Recovery Conference*, pages SPE–75138–MS.

Jerauld, G. (1997a). General three-phase relative permeability model for prudhoe bay. *SPE reservoir Engineering*, 12(04):255–263.

Jerauld, G. (1997b). General three-phase relative permeability model for prudhoe bay. *SPE reservoir Engineering*, 12(04):255–263.

Longe, P., Molomjav, S., Tsau, J.-S., Musgrove, S., Villalobos, J., D'Erasmo, J., Alhajeri, M. M., and Barati, R. (2025). Techno-economic evaluation of co2-eor and carbon storage in a shallow incised fluvial reservoir using captured-co2 from an ethanol plant. *Geoenergy Science and Engineering*, 246:213559.

Masalmeh, S., Farzaneh, A., and Sohrabi, M. (2025). Gas/co2 mobility under 2-phase and 3-phase flow in carbonate for co2-eor and ccs projects. In *IOR+ 2025-23rd European Symposium on IOR*, volume 2025, pages 1–23. European Association of Geoscientists & Engineers.

Mirzaei-Paiaman, A., Okuno, R., Lawal, T., Sheng, K., Chen, C., Lai, I., Chen, S., and Hu, L. (2024). Techno-economic-environmental analysis of co2 storage and eor in an underdeveloped field. In *SPE Improved Oil Recovery Conference?*, page D031S026R003. SPE.

Moulu, J., Vizika, O., Kalaydjian, F., and Duquerroix, J. (1997). A new model for three-phase relative permeabilities based on a fractal representation of the porous medium. In *SPE Annual Technical Conference and Exhibition?*, pages SPE–38891. SPE.

National Petroleum Council (2021). Meeting the dual challenge: A roadmap to at-scale deployment of carbon capture, use, and storage. Technical report, National Petroleum Council. Originally published December 2019, chapter last updated March 12, 2021.

Qi, R., LaForce, T. C., and Blunt, M. J. (2008). Design of carbon dioxide storage in oilfields. In *SPE Annual Technical Conference and Exhibition?*, pages SPE–115663. SPE.

Qi, R., LaForce, T. C., and Blunt, M. J. (2009). Design of carbon dioxide storage in aquifers. *International Journal of Greenhouse Gas Control*, 3(2):195–205.

Roussanaly, S. and Grimstad, A.-A. (2014). The economic value of co2 for eor applications. *Energy Procedia*, 63:7836–7843.

Schäfer, G., di Chiara Roupert, R., Alizadeh, A. H., and Piri, M. (2020). On the prediction of three-phase relative permeabilities using two-phase constitutive relationships. *Advances in Water Resources*, 145:103731.

Shahverdi, H. et al. (2012). *Characterization of three-phase flow and WAG injection in oil reservoirs*. PhD thesis, Heriot-Watt University.

Shahverdi, H. and Sohrabi, M. (2013). An improved three-phase relative permeability and hysteresis model for the simulation of a water-alternating-gas injection. *Spe Journal*, 18(05):841–850.

Shahverdi, H. and Sohrabi, M. (2015). Modeling of cyclic hysteresis of three-phase relative permeability during water-alternating-gas injection. *SPE Journal*, 20(01):35–48.

Shahverdi, H. and Sohrabi, M. (2017). A mechanistic model for prediction of three-phase flow in petroleum reservoirs. *Journal of Petroleum Science and Engineering*, 157:507–518.

Shu, D. Y., Deutz, S., Winter, B. A., Baumgärtner, N., Leenders, L., and Bardow, A. (2023). The role of carbon capture and storage to achieve net-zero energy systems: Trade-offs between economics and the environment. *Renewable and Sustainable Energy Reviews*, 178:113246.

Stone, H. (1970). Probability model for estimating three-phase relative permeability. *Journal of Petroleum Technology*, 22(02):214–218.

Stone, H. (1973). Estimation of three-phase relative permeability and residual oil data. *Journal of Canadian Petroleum Technology*, 12(04).

Whittaker, S. and Perkins, E. (2013). Technical aspects of co_2 enhanced oil recovery and associated carbon storage. Technical report, Global CCS Institute. Final Version.